A spiral structure in the disk of EX Draconis on the rise to outburst maximum

Raymundo Baptista

Departamento de Física, Universidade Federal de Santa Catarina, Campus Trindade, 88040-900, Florianópolis - SC, Brazil

bap@fsc.ufsc.br

and

M. S. Catalán

Department of Physics, Keele University, Keele, Staffordshire, ST5 5BG, UK

msc@astro.keele.ac.uk

ABSTRACT

We report on the R-band eclipse mapping analysis of high-speed photometry of the dwarf nova EX Dra on the rise to the maximum of the November 1995 outburst. The eclipse map shows a one-armed spiral structure of $\sim 180^{\circ}$ in azimuth, extending in radius from $R \simeq 0.2$ to $0.43~R_{\rm L1}$ (where R_{L1} is the distance from the disk center to the inner Lagrangian point), that contributes about 22 per cent of the total flux of the eclipse map. The spiral structure is stationary in a reference frame co-rotating with the binary and is stable for a timescale of at least 5 binary orbits. The comparison of the eclipse maps on the rise and in quiescence suggests that the outbursts of EX Dra may be driven by episodes of enhanced mass-transfer from the secondary star. Possible explanations for the nature of the spiral structure are discussed.

Subject headings: accretion, accretion disks – binaries: close – binaries: eclipsing – novae, cataclysmic variables – stars: individual: (EX Draconis)

1. Introduction

Dwarf novae are close binaries in which a late type star (the secondary) overfills its Roche lobe and transfers matter to a companion white dwarf via an accretion disk. They show recurrent outbursts of 2–5 magnitudes on timescales of days to several months, resulting either from an instability in the mass transfer from the secondary (the MTI model), or from a thermal instability in the accretion disk (the DI model) which switches the disk from a low to a high-viscosity regime (Warner 1995 and references therein). Observations of dwarf novae at the early phases of the outburst offer good prospects to discriminate between the two competing models. The MTI

model predicts that the accretion disk should shrink at the beginning of the outburst due to the sudden accretion of material with low angular momentum while the luminosity of the bright spot should increase in response to the higher mass-transfer rate (e.g. Warner 1995). No such effects are expected in the DI model. Most of the few current observations seem to support the DI model (e.g., Vogt 1983; Rutten et al. 1992a), although recent results suggest an MTI origin for the outbursts in the intermediate polar EX Hya (Hellier et al. 2000).

Spiral shocks have long been proposed as a possible mechanism for transport of angular momentum in accretion disks (e.g., Sawada, Matsuda & Hachisu 1986; Savonije, Papaloizou & Lin 1994) and may be the key, together with magnetic viscosity (Hawley, Balbus & Winters, 1999), in understanding the anomalous viscosity mechanism responsible for the spiraling inwards of the disk material. The recent discovery of spiral shocks in the accretion disk of the dwarf nova IP Pegasi in outburst (e.g., Steeghs, Harlaftis & Horne 1997; Baptista, Harlaftis & Steeghs 2000a) confirmed the results of hydrodynamical simulations (e.g., Stehle 1999) and boosted the research in this topic. Two-armed spiral shocks are excited in the outer regions of the disk by the tides raised by the secondary star when the outbursting accretion disk extends far enough into the Roche Lobe.

EX Draconis is a long period ($P_{orb} = 5$ hr) eclipsing dwarf nova, the outbursts of which have typical amplitudes of 2.0 mag, duration of $\simeq 10$ days, and recurrence timescale of about 20 days (Baptista, Catalán & Costa 2000b; hereafter BCC). The analysis of a set of light curves along the outburst cycle led BCC to conclude that the outbursts do not start in the outer disk regions. (i.e., they are inside-out outbursts). Recently, Joergens, Spruit & Rutten (2000) found evidence of spiral shocks in the accretion disk of EX Dra from Doppler tomography close to outburst maximum.

In this letter we report on the comparative analysis of the light curves of BCC during the early rise to outburst maximum with those of the quiescent state of the binary. Our results show that a one-armed spiral structure develops in the accretion disk of EX Dra on the rise to maximum. Section 2 describes the data analysis. The results are presented in section 3 and discussed in section 4.

2. Data Analysis

Our data are R band light curves obtained with the 0.9-m James Gregory Telescope at the University of St. Andrews in 1995. The reader is referred to BCC for a detailed description of the data set and of the reduction procedures. We collected three eclipse light curves of EX Dra on the rising branch of the 1995 November outburst (eclipse cycles 7812, 7813 and 7817), two days after the onset of the outburst and two days before the outburst maximum (outburst D of BCC; see their Fig. 1). The quiescent state is represented by four light curves (eclipse cycles 8007, 8008, 8011 and 8013), obtained on 1995 December 27-28, about 10 days after the end of the subsequent outburst (outburst E of BCC). In order to improve the signal-to-noise ratio and to reduce the influence of flickering, the individual light curves were combined to produce average eclipse light curves for the two observed states. For each light curve, we divided the

data into phase bins of 0.003 cycle and computed the median for each bin. The median of the absolute deviations with respect to the median for each bin was taken as the corresponding uncertainty. The light curves were phase folded according to the sinusoidal ephemeris of BCC,

$$T_{mid} = \text{HJD } 2448398.4530(\pm 1) + 0.20993698(\pm 4) E +$$

$$+(8.2 \pm 1.5) \times 10^{-4} \sin \left[2\pi \frac{(E - 968)}{7045}\right] d$$
 (1)

Out-of-eclipse brightness changes are not accounted for by the eclipse mapping method, which assumes that all variations in the eclipse light curve are due to the changing occultation of the emitting region by the secondary star. Orbital variations were therefore removed from the light curves by fitting a spline function to the phases outside eclipse, dividing the light curve by the fitted spline, and scaling the result to the spline function value at phase zero. This procedure removes orbital modulations with only minor effects on the eclipse shape itself.

We applied eclipse mapping techniques (Horne 1985; Rutten, van Paradijs & Tinbergen 1992b; Baptista & Steiner 1993) to our light curves to solve for a map of the disk brightness distribution and for the flux of an additional uneclipsed component in each case. The uneclipsed component accounts for all light that is not contained in the eclipse map in the orbital plane (i.e., light from the secondary star and/or a vertically extended disk wind). The reader is referred to Rutten et al. (1992b) and Baptista, Steiner & Horne (1996) for a detailed description of and tests with the uneclipsed component. For the reconstructions we adopted the default of limited azimuthal smearing of Rutten et al. (1992b), which is better suited for recovering asymmetric structures than the original default of full azimuthal smearing (see Baptista et al. 1996). Simulations that show the ability of the eclipse mapping method to reconstruct asymmetric structures such as spiral arms are presented and discussed by Baptista et al. (2000a). As our eclipse map we adopted a grid of 75×75 pixels centered on the primary star with side 2 R_{L1}, where R_{L1} is the distance from the disk center to the inner Lagrangian point. The eclipse geometry is defined by the mass ratio q and the inclination i. We adopted the parameters of BCC, q = 0.72and $i = 85^{\circ}$, which correspond to an eclipse width of the disk center of $\Delta \phi = 0.1085$. These combination of parameters ensure that the white dwarf is at the center of the map.

The statistical uncertainties of the eclipse maps were estimated with a Monte Carlo procedure (e.g., Rutten et al. 1992). A set of 20 artificial light curves is generated, in which the data points are independently and randomly varied according to a Gaussian distribution with standard deviation equal to the uncertainty at that point. The light curves are fitted with the eclipse mapping algorithm to produce a set of randomized eclipse maps. These are combined to produce an average map and a map of the residuals with respect to the average, which yields the statistical uncertainty at each pixel.

3. Results

The data and the model light curves are shown in the left-hand panels of Fig. 1. Horizontal dashed lines indicate the uneclipsed component in each case. The middle panels show the

corresponding eclipse maps in the same logarithmic grayscale. The maps in the right-hand panels show the asymmetric part of the maps in the middle panels and are obtained by calculating and subtracting azimuthally-averaged intensities at each radius.

The uneclipsed fluxes are 1.45 and 1.6 mJy, respectively, for the light curves in quiescence and during the rise. The uneclipsed component in quiescence is mostly due to the contribution of the secondary star to the R band flux, and is comparable to the quiescent mid-eclipse flux. The larger uneclipsed flux during the rise is possibly the result of additional emission from a (variable) vertically-extended disk wind component, which becomes non-negligible during the outbursts (see Baptista & Catalán 2000).

The light curve in quiescence shows a flat-bottomed asymmetric eclipse that is the result of the almost total occultation of a bright source at disk center and of a faint compact bright spot at disk rim. The spot in the eclipse map lies along the gas stream trajectory and yields a quiescent disk radius of $R_q = 0.51 \pm 0.02~R_{L1}$, in good agreement with the value measured by BCC. The width of the eclipse in the rise light curve is the same as in quiescence but the eclipse is skewed towards later phases, indicating the occultation of an asymmetric brightness distribution in the trailing side of the disk. The resulting eclipse map has a symmetrical, centered brightness distribution, and an asymmetric structure in the form of a spiral arm that is clearly visible in the right-hand panel of Fig. 1. The eclipse maps obtained with the Monte Carlo procedure consistently show a similar spiral structure. The asymmetric arc contributes about 22 per cent of the total flux of the eclipse map.

In order to trace the distribution in radius and azimuth of the asymmetric structures, we divided the eclipse maps in azimuthal slices (i.e., 'slices of pizza') and computed the distance at which the intensity is a maximum for each azimuth. We restricted the search to radii $R > 0.2 R_{L1}$ in order to avoid being affected by the central brightness source. The results are plotted in Fig. 2 as a function of binary phase (binary phases increase clockwise in the eclipse maps of Fig. 1 and phase zero coincides with the inner Lagrangian point L1). The lower panel shows the dependency of the maximum intensity with binary phase, while the upper panel gives the radial position of the maximum intensity as a function of binary phase (only the regions for which the radius of maximum intensity is larger than $0.2 R_{L1}$ are shown). The error bars were derived via Monte Carlo simulations with the eclipse light curves (section 2).

There are clear differences between the asymmetric structures in quiescence and on the rise to maximum. The quiescent bright spot is a well defined, compact source with narrow azimuthal $(\Delta\phi\simeq30^\circ)$ and radial $(\Delta R=0.04~R_{L1})$ extents. On the other hand, the asymmetric structure on the rise map is extended both in azimuth $(\Delta\phi\sim180^\circ)$ and radius (from $R\simeq0.2$ to 0.43 R_{L1}), showing a spiral pattern in which the radius of the maximum intensity continuously increases with binary phase. An estimate of the disk radius at the rising stage can be obtained from the outer radius of the spiral arm, $R_r=0.43~R_{L1}$.

We computed equivalent Keplerian velocities along the spiral structure by assuming $M_1 = 0.75 \pm 0.15 M_{\odot}$ and $R_{\rm L1} = 0.85 R_{\odot}$ (BCC). We obtain velocities in the range $600 - 800 \,\rm km\,s^{-1}$, larger than the velocities ($400 - 600 \,\rm km\,s^{-1}$) inferred for the spirals seen close to outburst maximum (Joergens et al. 2000). Since the eclipse map and the Doppler tomogram correspond

to different outburst stages, we are not able to distinguish whether the different velocities are the consequence of different radii for the spirals, or if they are the signature of sub-Keplerian velocities in spiral shocks – as seen in IP Peg (Baptista et al. 2000a).

4. Discussion

Figures 1 and 2 show that the spiral arm is brighter and closer to disk center than the quiescent bright spot. The ratio of the intensity of the outer parts of the spiral arm and that of the quiescent bright spot ($\simeq 3.5$, lower panel of Fig. 2) is much larger than the expected increase in accretion luminosity owing to the reduction in radius (for a constant mass accretion rate), $L_{acr}(R_r)/L_{acr}(R_q) = R_q/R_r = 1.2$. This discrepancy indicates that the mass accretion rate on the rise to maximum is larger than the mass inflow at the quiescent bright spot by a factor of $\simeq 3^1$. Moreover, if the outer radius of the spiral arm can be assigned to the disk radius, the comparison of R_q and R_r indicates that the accretion disk shrinks at the onset of the outburst. This result is in agreement with the predictions of the MTI model (Warner 1995), and suggests that the outburst in EX Dra is driven by a burst of enhanced mass-transfer from the secondary star.

We now turn our attention to the nature of the observed asymmetric structure. It is hard to understand the observed one-armed spiral structure in terms of tidally-induced spiral shocks. First, because the accretion disk radius at the corresponding outburst stage (again assumed to be of the same order of the outer radius of the spiral arm, $R_r = 0.43 R_{L1}$) is significantly smaller than the range in radius $(0.56 - 0.75 R_{L1})$ required to excite spiral shocks strong enough to be observed (Steeghs & Steele 1999). Secondly, because the tidal effect of the secondary star should, in principle, lead to the formation of a two-armed spiral structure (e.g., Yukawa, Boffin & Matsuda 1997; Armitage & Murray 1998), instead of the observed one-armed spiral.

An alternative explanation for the spiral structure in terms of enhanced gas stream emission might be advocated, although the position of the spiral arm is clearly not consistent with the location of the gas stream trajectory (see Fig.1). Inconsistently low mass ratios ($q \lesssim 0.1$) would be required to bring the gas stream trajectory in closer agreement with the observed spiral pattern. If valid, this alternative would also indicate an MTI origin for the outbursts of EX Dra.

A third explanation may be devised if we note that outbursting accretion disks might depart from the geometrically thin disk approximation. At the high inclination of EX Dra, this may have important effects on the eclipse maps. It may be possible that the observed spiral pattern is the combination of emission from a bright spot/stream running along the edge of the disk and the (apparently) enhanced emission from the far (with respect to the secondary star) side of a flared accretion disk. This scenario makes the bright spot on the rise a factor of 3 brighter than the quiescent bright spot, also in agreement with the predictions of the MTI model.

¹In fact, this is a lower limit, since the bulk of the accretion luminosity at the smaller R_r radius should move to shorter wavelengths due to the higher effective temperature, making the ratio of intensities in the R-band $I_{\nu}(R_r)/I_{\nu}(R_q) < L_{acr}(R_r)/L_{acr}(R_q)$.

The observed spiral structure bears resemblance with the transient arc-shaped asymmetric structures seen in 2-D and 3-D numerical simulations of accretion flows, at the onset of mass transfer (Makita, Miyawaki & Matsuda 1998; Makita & Matsuda 1998) or at the start of an instability-driven outburst (Różyczka & Spruit 1993). In this regard, useful constraints on future numerical simulations attempting to reproduce the observed spiral pattern may be obtained by noting that the individual light curves combined to produce the average rise light curve cover a time interval of 5 binary cycles. Their eclipse shape is the same under the uncertainties. Hence, the spiral structure seems to be stationary on a reference frame co-rotating with the binary and stable for a time length of, at least, 5 binary orbits.

Finally, we note that, contrary to the usual assumption, inside-out outbursts are not necessarily inconsistent with the MTI model, provided that the burst of mass transfer leads to the formation of a spiral structure well inside the primary lobe, that expands thereafter both inwards and outwards under the effects of mass and angular momentum redistribution to form a fully developed accretion disk.

We thank Emilios Harlaftis for helpful discussions and comments which stimulated the writing of this paper. This work was partially supported by the PRONEX/Brazil program through the research grant FAURGS/FINEP 7697.1003.00. RB acknowledges financial support from CNPq/Brazil through grant no. 300354/96-7. MSC acknowledges financial support from a PPARC post-doctoral grant during part of this work.

REFERENCES

Armitage, P. J. & Murray, J. R. 1998, MNRAS, 297, L81

Baptista, R. & Catalán, M. S. 2000, MNRAS, submitted

Baptista, R., Harlaftis, E. T. & Steeghs, D. 2000a, MNRAS, 314, 727

Baptista, R., Catalán, M. S. & Costa, L. 2000b, MNRAS, in press (astro-ph/0002382) [BCC]

Baptista, R. & Steiner, J. E. 1993, A&A, 277, 331

Baptista, R., Steiner, J. E. & Horne, K. 1996, MNRAS, 282, 99

Hawley, J. F., Balbus, S. A. & Winters, W. F. 1999, ApJ, 518, 394

Horne, K. 1985, MNRAS, 213, 129

Hellier, C., et al. 2000, MNRAS, in press (astro-ph/0001430)

Joergens, V., Spruit, H. C. & Rutten, R. G. M. 2000, A&A, in press (astro-ph/0002302)

Makita, M., Miyawaki, K. & Matsuda, T. 1998, preprint (astro-ph/9809003)

Makita, M. & Matsuda, T. 1999, in proc. International Conference on Numerical Astrophysics, eds. S. M. Miyama et al. (Boston: Kluwer Academics), 227 (astro-ph/9807237)

Różyczka, M. & Spruit, H. C. 1993, ApJ, 417, 677

Rutten, R. G. M., Kuulkers, E., Vogt, N. & van Paradijs, J. 1992a, A&A, 254, 159

Rutten, R. G. M., van Paradijs, J. & Tinbergen, J. 1992b, A&A, 260, 213

Savonije, G. J., Papaloizou, J. & Lin, C. 1994, MNRAS, 268, 13

Sawada, K., Matsuda, T. & Hachisu, I. 1986, MNRAS, 219, 75

Steeghs, D., Harlaftis, E. T. & Horne, K. 1997, MNRAS, 290, L28

Steeghs, D. & Stehle, R. 1999, MNRAS, 307, 99

Stehle, R. 1999, MNRAS, 304, 687

Vogt, N. 1983, A&A, 129, 29

Warner, B. 1995, Cataclysmic Variable Stars, Cambridge Astrophysics Series 28 (Cambridge: Cambridge University Press)

Yukawa, H., Boffin, H. M. J. & Matsuda, T. 1997, MNRAS, 292, 321

This preprint was prepared with the AAS LATEX macros v5.0.

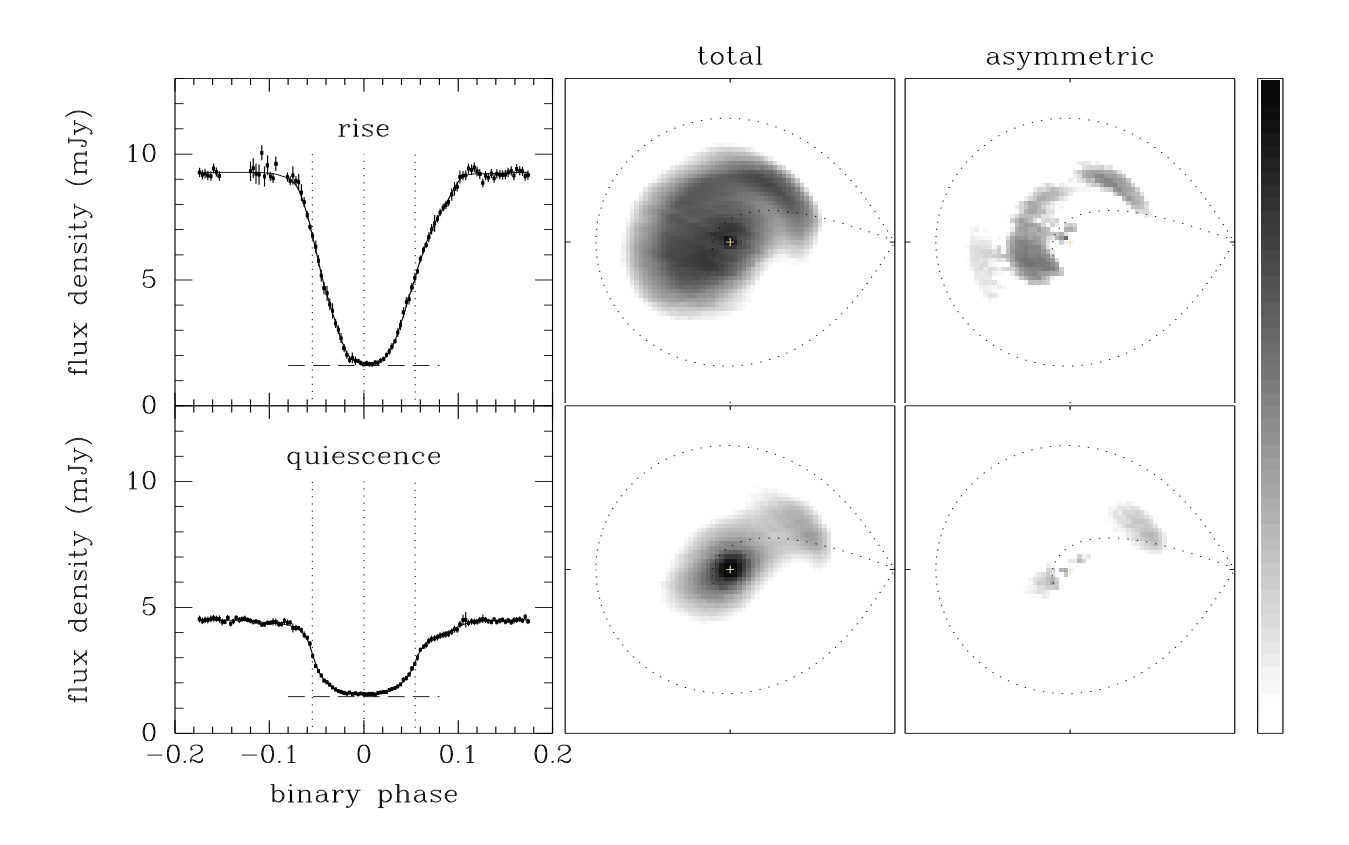


Fig. 1.— Left: Data (dots with error bars) and model (solid lines) light curves of EX Dra on the rise to maximum and in quiescence. Vertical dotted lines mark mid-eclipse and the ingress/egress times of the white dwarf. Horizontal dashed lines indicate the uneclipsed component in each case. Middle: eclipse maps in a logarithmic grayscale. Right: the eclipse maps of the middle panel after subtracting their symmetric part; these diagrams emphasize the asymmetric structures. Brighter regions are indicated in black; fainter regions in white. A cross mark the center of the disk; dotted lines show the Roche lobe and the gas stream trajectory; the secondary is to the right of each map and the stars rotate counterclockwise.

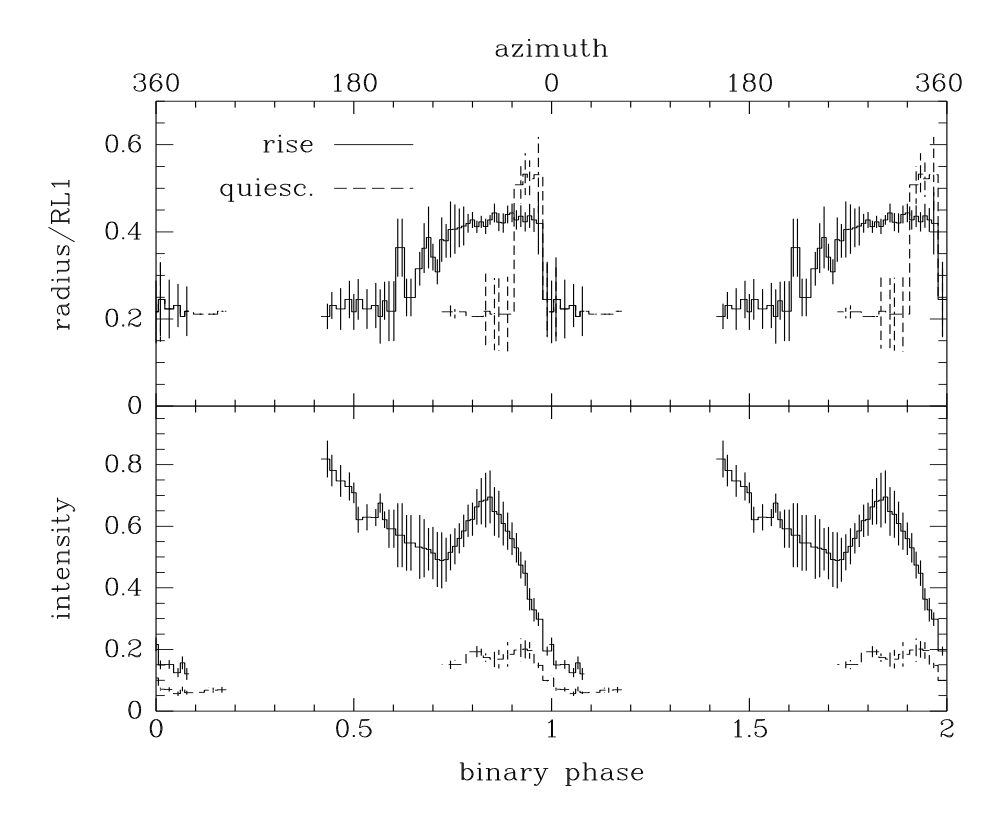


Fig. 2.— The dependency with binary phase of the maximum intensity and radius at maximum intensity, as derived from the eclipse maps on the rise (solid) and quiescence (dashed). The intensities are plotted in an arbitrary scale.